We are IntechOpen, the world's leading publisher of Open Access books Built by scientists, for scientists

4,800
Open access books available

122,000
International authors and editors

135M
Downloads

Our authors are among the

154
Countries delivered to

TOP 1%
most cited scientists

12.2%
Contributors from top 500 universities

CLARIVATE ANALYTICS BOOK CITATION INDEX INDEXED

WEB OF SCIENCE™

Selection of our books indexed in the Book Citation Index in Web of Science™ Core Collection (BKCI)

Interested in publishing with us?
Contact book.department@intechopen.com

Numbers displayed above are based on latest data collected.
For more information visit www.intechopen.com

7

Producing Poly-Silicon from Silane in a Fluidized Bed Reactor

B. Erik Ydstie and Juan Du
Carnegie Mellon University
USA

1. Introduction

The accumulated world solar cell capacity was 2.54 GW in 2006, 89.9% based on mono- or multi-crystalline silicon wafer technology, 7.4% thin film silicon, and 2.6% direct wafering (Neuhaus & Münzer, 2007). The rapidly expanding market and high cost of silicon led to the development of thin-film technologies such as the Cadmium Telluride (CdTe), Copper-Indium-Gallium Selenide (CIGS), Dye Sensitized Solar Cells, amorphous Si on steel and many other. The market share for thin-film technology jumped to nearly 20% of the total 7.7 GW of solar cells production in 2009 (Cavallaro, 2010).

There are more than 25 types of solar cells and modules in current use (Green & Emery, 1993). Technology based on mono-crystalline and multi-crystalline silicon wafers presently dominate and will probably continue to dominate since raw material availability is not a problem given that silicon is abundant and cheap. Solar cells based on rare-earth metals pose a challenge since the cost of the raw materials tend to fluctuate and availability is limited. However the cost of silicon solar cells and the raw material, solar grade poly-silicon is too high and this technology will be displaced unless cost effective alternatives are found to make silicon solar cells.

Figure 1 shows the approximate distributions for the different costs in producing a silicon based solar module (Muller et al., 2006). The figure shows where there is significant incentive to reduce costs. The areas of solar grade silicon (SOG) production and wafer manufacture stand out. These processes are presently not well optimized and many opportunities exist to improve the manufacturing technology through process innovation, retro-fit, optimization and process control.

Poly-silicon, the feedstock for the semiconductor and photovoltaic industries, was in short supply during the beginning of the last decade due to the expansion of the photovoltaic (PV) industry and limited recovery of reject silicon from the semiconductor industry. The relative market share of silicon for the electronic and solar industries is depicted in Figure 2. This figure shows the growing importance of the the solar cell industry in the poly-silicon market. Take last year as an example, a total amount of 170,000 metric tons of poly-silicon was produced and 85% was consumed by solar industry while only 15% was consumed by the semiconductor industry. This represents a complete reversal of the situation less than two decades ago. During the last decade, the total PV industry demand for feedstock grew by more than 20% annually. The forecasted growth rate for the next decade is a conservative 15% per year. The available silicon capacities for both semiconductor and PV industry are limited to 220,000 metric tons for the time being.

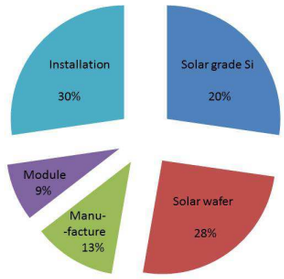

Fig. 1. The cost distribution of a silicon solar module.

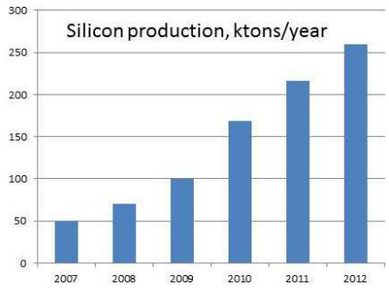

Figure I: Silicon production per year

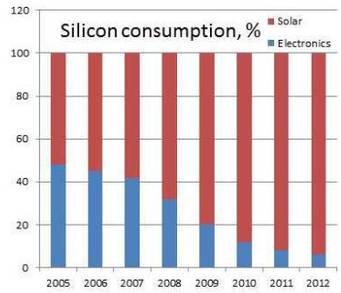

Figure II: Consumption percentage of solar and electronics

Fig. 2. Poly-Silicon Production and consumption for Electronic and PV Industries (Fishman, 2008).

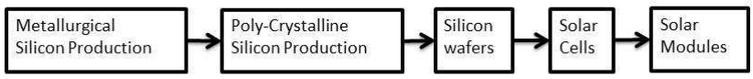

Fig. 3. The supply chain for solar cell modules.

Six companies supplied most of the poly-silicon consumed worldwide in the year of 2000, namely, REC Silicon, Hemlock Semi-Conductor, Wacker, MEMC, Tokuyama and Mitsubishi (Goetzberger et al., 2002). Those companies still cover most of the world wide production capacity and produced over 75% of the poly-silicon in 2010.

2. Solar grade poly-silicon production

Figure 3 illustrates the typical silicon solar cell production. The supply chain starts with the carbothermic reduction of silicates in an electric arc furnace. In this process large amounts of electrical energy breaks the silicon-oxygen bond in the SiO_2 via the endothermic reaction with carbon. Molten Si-metal with entrained impurities is withdrawn from the bottom of the furnace while CO_2 and fine SiO_2 particles escape with the flu-gas (Muller et al., 2006).

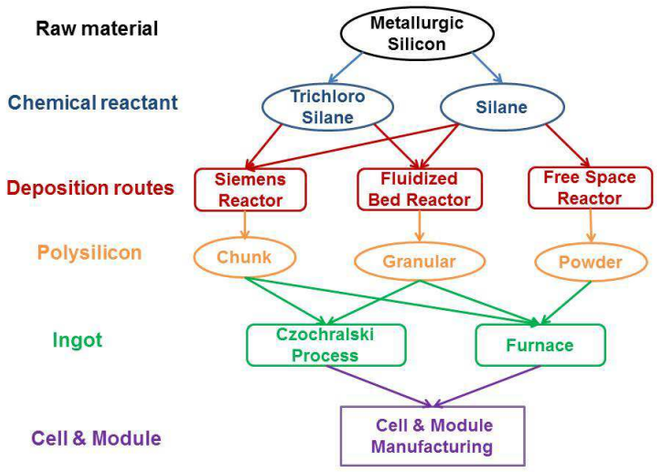

Fig. 4. Silicon based Solar Cell Production Process.

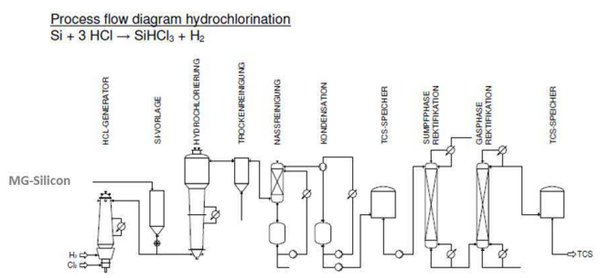

Fig. 5. The production of highly pure TCS from MG-Si.

Metallurgical grade silicon (MG-Si) at about 98.5-99.5% purity is sold to many different markets. The majority of MG-Si is used for silicones and aluminum alloys (Surek, 2005). A much smaller portion is for fumed silica, medical and cosmetic products and micro-electronics. A small but rapidly growing proportion is used for solar applications.

Metallurgical silicon is converted to high-purity poly-silicon through two distinct routes. In the metallurgical route the silicon is purified through a combination of steps targeted at different impurities (Muller et al., 2010). Leaching with calcium based slags may remove some impurities whereas directional solidification takes advantage of the high liquid-solid segregation coefficient of metallic impurities and leaching eliminates metallic silicides in the grain boundaries. One bottleneck of this process is low purity and yield relative to the chemical route. Only a small percentage of the current market is based on this approach (Fishman, 2008).

High purity poly-silicon suitable for solar cells and micro-electronics can also be produced by a chemical route which typically proceeds in two steps. In the first step MG-Si reacts with HCl to form a range of chlorosilanes, including tri-chlorosilane (TCS). TCS has a normal boiling point of 31.8^{o}C so that it can be purified by distillation. One process alternative for producing TCS is shown in Figure 5. Poly-silicon is then produced in the same manufacturing facility by pyrolysis of TCS in reactors that are commonly referred to as Bell or Siemens reactors (del Coso et al., 2007). In the Bell reactor TCS passes over high purity silicon starter rods which are

heated to about 1150^oC by electrical resistance heating. The gas decomposes as

$$2HSiCl_3 \rightarrow Si + 2HCl + SiCl_4$$

Silicon deposits on the silicon rods as in a chemical vapor deposition process. 9N(99.999999999%) silicon is used for micro-electronics applications. Silicon which is 6N or better is called solar grade silicon (SOG-Si) and it can be used to produce high quality solar cells (Talalaev, 2009).
The free space reactor provides an alternative to the Siemens reactor. It has lower capital and operating cost. However, its disadvantage is that it is difficult to regulate the melting process to generate ingots and wafers. This process has not been used industrially on a large scale yet (Fishman, 2008).
The annual price for solar grade silicon went through a very sharp maximum in 2008 due to high demand and limited poly-silicon production capacity. The increase in price was expected (Woditsch & Koch, 2002) and led to a similar increase in the cost of wafers. The price of solar grade silicon is expected to stabilize in the coming decade as new technologies are introduced and capacity is added to the supply chain: The classical TCS process was designed for micro-electronics manufacture where silicon cost is not as critical as in the solar cell industry. Some companies have retro-fitted their processes to produce solar rather than micro-electronics grade silicon. The pyrolysis process has been made suitable for high volume production of poly-silicon; reactive separation and complex instead of simple distillation has been proposed to reduce energy requirements; and fluid bed reactor technology is set to replace the Bell reactors during the next decade. Finally, progress has been made in making solar grade silicon directly using metallurgical routes. All attempts have not been as successful as was hoped for yet. Nevertheless, it is very likely that solar grade silicon prices can be reduced to $25-30 per kg in the next decade if the tempo of industry expansion is maintained (Neuhaus & Münzer, 2007).

3. Fluidized bed reactor

Fluidized bed reactors have excellent heat and mass transfer characteristics and can be utilized for Silane decomposition to overcome the energy waste problem in Siemens process. The energy consumption is reduced because the decomposition operates at a lower temperature and cooling devices are not required. In addition fluidized beds have high throughput rate and operate continuously reducing further capital and operating costs. The final product consist of small granules of high purity silicon that are easy to handle compared to powder produced by free space reactor (Odden et al., 2005).
In the fluidized bed reactor (Kunii & Levenspiel, 1991), the reactive gas is introduced into the reactor together with preheated fluidizing gases, such as hydrogen or helium. Heat for the thermal decomposition is supplied by external heating equipment. Pyrolysis of silicon containing gas produces silicon deposition on seed particles, the subsequent particle growth is due to heterogeneous chemical vapor deposition as well as scavenging of homogeneous silicon nuclei. This results in a high deposition rate by a combination of heterogeneous and homogeneous decomposition reactions. As the silicon seed particles grow, the larger particles move to the lower part of the bed and are removed as a final product. The continuous removal of silicon seed particles after they have grown to the desired size leads to depletion of particles and it is necessary to introduce additional silicon seed particles into the fluidized bed to replace those removed final product (Würfel, 2005).
Two techniques are used to provide a continuous supply of pure silicon seed particles to the fluidized bed reactor. One technique uses a hammer mill or roller crushers to reduce

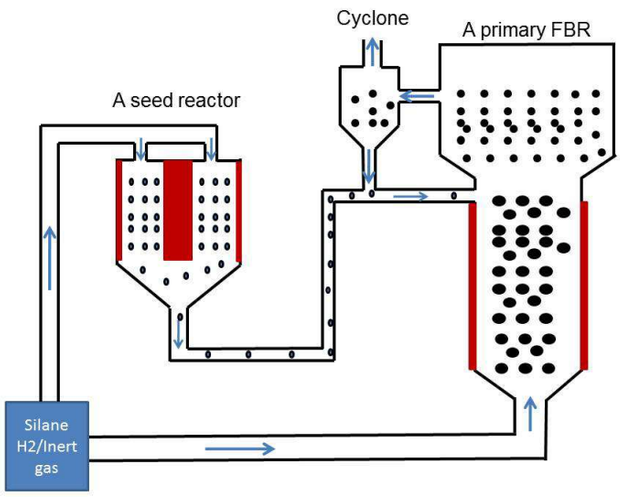

Fig. 6. Fluidized bed reactor with seed generator.

the bulk silicon to a specific particle size distribution suitable for use as seed particles. However, this technique is expensive and causes severe contamination problems. Moreover, the crushing results in a non-spherical seed particle which presents an undesired surface for silicon deposition. The other technique for producing silicon seed particles involves the recycling small particles generated in and removed from the fluidized bed (Odden et al., 2005). In the fluidized bed, the majority of silicon produced during thermal decomposition undergoes heterogeneous deposition on the surface of the seed while a certain amount of silicon is formed homogeneously as gas dust recycled back into the reactor as seed particles (Caussat et al., 1995a). However, those amount of silicon is not sufficient to meet the entire demand for new seed particles. The combination of the recycled homogeneous particles and seed particles produced by crushing (Kojima & Morisawa, 1991) can provide an effective means of re seeding. More importantly, these homogeneously formed particles are amorphous such that they do not provide desirable surface for deposition neither.

A novel seed generator for continuously supplying silicon seed particles solves the above problems (Hsu et al., 1982). This seed generator produces precursor silicon seed via thermal decomposition of silicon containing gas. This device generates uniformly shaped seed particles with desirable fluidization characteristics and silicon deposition. The scheme of silicon production process is illustrated in Figure 6. It comprises a primary fluidized bed reactor and a silicon seed generator. The seed particles are introduced into the primary fluidized bed reactor through seed particle inlet (Steinbach et al., 2002).

4. Silane pyrolysis in fluidized beds

Hogness *et al.* (Hogness et al., 1936) was one of the earliest to undertake a series of experiments to study the thermal decomposition of silane. They concluded that the reaction was homogeneous and first order. The hydrogen acted as an inhibitor for the decomposition and no reactions between hydrogen and silicon to form silane was observed. Zambov (Zambov, 1992) investigated the kinetics of homogeneous decomposition of silane and their experimental results showed that homogeneous and heterogeneous pyrolysis coexisted. Furthermore they developed a mathematical model to demonstrate that the ratio of

homogeneous decomposition to heterogeneous deposition grew with increasing temperature and pressure and thus resulted in a substantial degradation of the layer thickness uniformity. A suitable model for silane pyrolysis was developed by Lai *et al.* (Lai et al., 1986) to describe different reaction mechanisms in fluidized bed reactors. They assumed that silane decomposed by heterogeneous and homogeneous decomposition, and occurred via seven pathways as following:

1. Chemical vapor deposition on silicon particles (heterogeneous deposition);
2. Chemical vapor deposition on fines (heterogeneous deposition);
3. Homogeneous decomposition to form Silicon vapor;
4. Coalescence of formation of fines;
5. Diffusion-aided growth of fines;
6. Growth of fines by coagulation;
7. Scavenging of fines by particles;

Heterogeneous decomposition of silane on the existing silicon seed particles (pathway 1) or on the formed nuclei (pathway 2) lead to a chemical vapor deposition of silicon. The reaction rate was described by first order form published by Iya *et al.* (Iya et al., 1982).
Homogeneous decomposition forms a gaseous precursor (pathway 3) that nucleate a new solid phase of silicon, which is called silicon vapor. The concentration of vapor given by Hogness (Hogness et al., 1936) and Caussat (Caussat et al., 1995b) was always negligible as they can be suppressed by diffusion aided growth and coalescence of fines.
By pathway 4 nucleation of critical size nuclei, occurs whenever supersaturation is exceeded. The concentration of silicon vapor can be suppressed by diffusion and condensation on large particles (pathway 5). We assume here that nucleation occurs by the homogeneous nucleation theory. The molecular bombardment rate of small particles (pathway 4) is calculated by the classical expression of kinetic theory while the diffusion rate to large particles (pathway 6) is readily obtained from film theory of mass transfer. The coagulation rate of the fines in pathway 6 was determined by the coagulation coefficient which only depend on the average size of the fines. Scavenging rate was also proportional to a scavenging coefficient depending on the size of particles. Those seven pathways are widely used in practice to describe the reaction mechanism to produce silicon from silane.
Two significant problems exist for industrial practice: fines formation and particle agglomeration (Cadoret et al., 2007). For the problem of fines formation, their experimental study showed that for the inlet concentration of the reactive gas less than 20%, silane conversion was quite complete and fines formation limited. The fines ratio never exceeded 3% regardless of inlet concentration of silane. This encouraging result demonstrated that silicon chemical vapor deposition on powders in a fluidized bed was possible and efficient. The other new observation that chemical reactions of gaseous species on cold surfaces was the cause of fines formation was in complete contradiction with previous works (Hsu et al., 1982) (Lai et al., 1986), for which fines were formed homogeneously in fluidized bed. As to the problem of particle agglomeration, they observed that the presence of silane in the reactor could modify particle cohesiveness. The more plausible explanation for this modification was the reactive species adsorbed on particle surfaces could act as a glue for solids (Caussat et al., 1995a).

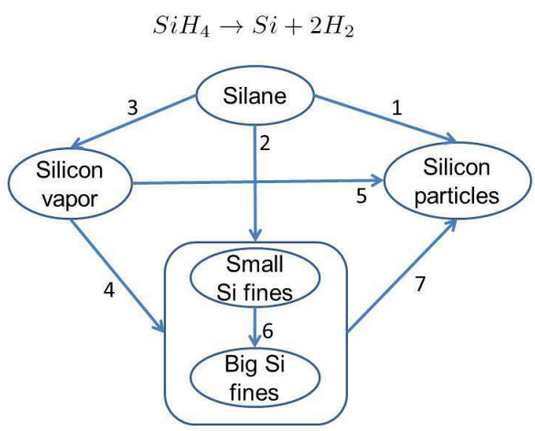

Fig. 7. Reaction pathways for conversion of silane to silicon. (Lai et al., 1986)

5. Computational fluid dynamics modeling

Computational fluid dynamics offers a powerful approach to understanding the complex phenomena that occur between the gas phase and the particles in the fluidized bed. The Lagrangian and Eulerian models have been developed to describe the hydrodynamics of gas solid flows for the multiphase systems (Piña et al., 2006). The Lagrangian model solves the Newtonian equations of motion for each individual particle in the gas solid system. However the large number of equations cause computational difficulties to simulate industrial fluidize beds reactors. The Eulerian model treats all different phases as continuous and fully interpenetrating. Generalized Navier-Stokes equations are employed for the interacting phases.

Constitutive equations are necessary to close the governing relations and describe the dynamics of the solid phase. To model solid particles as a separated phase, granular theory is employed to determine its physical parameters. The highly reduced number of equations in the Eulerian model needs much less effort to solve in comparison to the Lagrangian model. Modeling the hydrodynamics of gas-solid multiphase systems with Eulerian models has shown a promising approach for fluidized bed reactors.

Commercial software has been used to solve the models mentioned above. FEMLAB solves the partial differential equations by simulating fluidized bed reactors (Balaji et al., 2010). The simulations account for dynamic transport and hydrodynamic phenomena. Mahecha-Botero *et al.* (Mahecha-Botero et al., 2005) presented a generalized dynamic model to simulate complex fluidized bed catalytic systems. The model describes a broad range of multi-phase catalytic systems subject to mass and energy transfer among different phases, changes in the molar/volumetric flow due to the reactions and different hydrodynamic flow regimes. The generalized model (Mahecha-Botero et al., 2006) dealt with anisotropic mass diffusion and heat conduction and was used for different flow regimes which included bubble phase, emulsion phase and freeboard. The model was applied to simulate an oxychlorination fluidized bed reactor for the production of ethylene dichloride from ethylene. An exchange term was introduced to simulate the fluidized bed reactor as interpenetrating continua, composed of two interacting phases. The numerical results were very similar to those of Abba *et al.* (Abba et al., 2002) and gave good agreement with industrial reactor measured results.

Guenther *et al.* (Guenther et al., 2001) presented an althernative method for simulating fluidized bed reactors using the computational codes MFIX (Multiphase Flow with Interphase eXchanges) developed at the US Department of Energy National Energy Technology Laboratory. Three-dimensional simulations of silane pyrolysis were carried out by using MFIX. The reaction chemistry was described by the homogeneous and heterogeneous reactions described above. The results showed excellent agreement with experimental measurements and demonstrated that these methods can predict qualitatively the dynamical behavior of fluidized bed reactors for silane pyrolysis. Caussat *et al.* (Cadoret et al., 2007) used MFIX for transient simulations for silicon fluidized bed chemical vapor deposition from silane on coarse powders. The three-dimensional simulations provided better results than two-dimension simulations. The model predicts the temporal and spatial evolutions of local void fractions, gas and particle velocities and silicon deposition rate.
White *et al.* (White, 2007) used FLUENT to capture the dynamics of gas flow through a bed of particles with one constant average size. The inputs to FLUENT were reactor geometry, gas flow rates and temperature, heater duty, particle hold-up and average size. The CFD calculations predicted the bed properties such as the overall bed density and the temperature as functions of height. This study formed the basis for a multi-scale model for silane pyrolysis in FBR (Du et al., 2009)

6. The dynamics of particulate phase

Fluidized bed reactor dynamics are characterized by the production, growth and decay of particles contained in a continuous phase. Such dynamics can be found everywhere in the chemical engineering field, such as crystallization, granulation and fluidized bed vapor decomposition. Particularly for the solar grade silicon production process in a fluidized bed, the particles grow with heterogeneous chemical vapor deposition and homogeneous decomposition. White *et al.* (White et al., 2006) developed a dynamical model to represent the size distribution for silicon particles growth. The idea for the model development is based on classical population balance proposed by Hulburt and Katz (Hulburt & Katz, 1964). Hulburt *et al.* used the theory of statistical mechanics to develop an infinite dimensional phase space description of the particle behavior. The resulting balance equations express the conservation of probability in the phase space. A set of integro-partial differential equations are generated if the population balance is incorporated with mass balance for the continuous phase. However it requires significant computational efforts to solve those equations. Moment transformation and discretization are two commonly used methods to solve those equations. Randolph and Larson (Randolph & Larson, 1971) proposed the use of moment transformation while Clough (Cooper & Clough, 1985) used orthogonal collocation. Hounslow (Hounslow, 1990) and Henson *et al.* (Henson, 2003) employed various discretization techniques to solve them.
Du *et al.* (Du et al., 2009) reduced the continuous population balance to finite dimensional space by discretizing the size of particles into a finite number of size intervals. In each size interval, both mass balance and number balance are established and the discrete population balance is obtained by comparing those two balance equations. This approach ensures that conservation laws are maintained at all discretization levels and facilitates computation without additional discretization.
Figure 8 illustrates the modeling approach developed by White *et al.* and how it describes how particles change as a function of time. In this method particles are distributed among N discrete size intervals, characterized by an average mass m_i for $i = 1, ..., N$. The relationship between the total mass of particles (M_i) in an interval and the number of particles in each

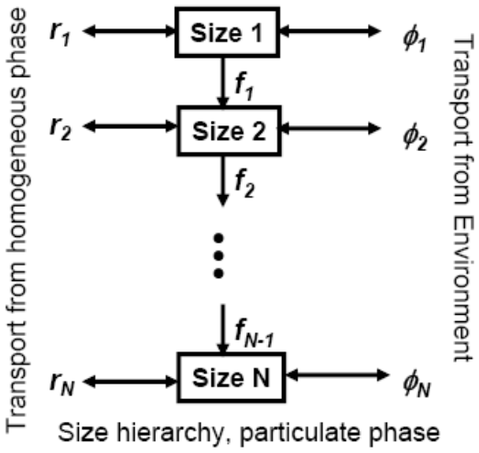

Fig. 8. The network representation of population balance

interval (n_i) is thereby given by the expression

$$M_i = m_i n_i. \tag{1}$$

The mass balance for size interval i is written

$$\frac{dM_i}{dt} = q_i + r_i + f_{i-1} - f_i + f_i^a \tag{2}$$

The rate of addition of particles to interval i from the environment is q_i^{in} while particle withdrawal is q_i^{out}, so the total external flow of particles is represented by

$$q_i = q_i^{in} - q_i^{out}.$$

The rate of material transfer from the fluid phase to the particle is represented by r_i. The term, f_i^a represents the rate of change due to agglomeration, breakage or nucleation. The value can be expressed so that

$$f_i^a = f_i^{a,in} - f_i^{a,out},$$

where $f_i^{a,in}$ represents particle transition to interval i due to agglomeration or nucleation, and $f_i^{a,out}$ represents particle transition out of an interval due to breakage or agglomeration. These terms are often referred to as birth and death in the population balance literature. Finally, the rate of transition of particles from one size interval to the next, caused by particle growth, is represented by f_{i-1} for flow into interval i and f_i for flow out of interval i. By connecting several of these balances together we get the network description of the particulate system illustrated in Figure 8. The model was validated by experimental data from pilot plant tests (**?**) and it was used for pilot plant design and scale-up. It also was used for further development of control strategies and study of dynamical stability of particles' behavior in fluidization processes.

7. Multi-scale modeling

Du *et al.* (Du et al., 2009) proposed a multi-scale approach for accurate modeling of the entire process. The hydrodynamics were modeled using CFD, which provides a basis for a simplified reactor flow model. The kinetic terms and the reactor temperature and concentrations are expressed as functions of reactor dimensions, void volume and time in the CFD module. Reactor temperature and concentration from the CFD module provides inputs to the CVD module. The CVD module calculates the overall process yield which provided an input to the population balance module. The average particle diameter is then calculated by population balance module and imported into the CFD module to complete model integration. In continuation of the above mentioned works by White *et al.* (White et al., 2007), Balaji *et al.* (Balaji et al., 2010) presented the complete multi-scale modeling approach including the effect of computational fluid dynamics along with population balance and chemical vapor deposition models. For the first time in the field of silicon production using fluidized beds, they coupled all the effects pertaining to the system (using partial differential equations (CFD), ordinary differential equations (PBM) and algebraic equations (CVD)) and they solved the resulting nonlinear partial differential algebraic equations with a computationally efficient and inexpensive solution methodology.
In order to verify the multi-scale model, we compare the numerical results with experimental data. The relationship between particle flow rates and average particle size at steady state is derived as (White, 2007),

$$1 + \frac{P}{S} = \frac{n_p}{n_s}\left(\frac{D_{ap}}{D_{as}}\right)^3 \tag{3}$$

where P is the product withdraw flow rate and S is the seed addition rate. D_{ap} is the average particle diameter of product and D_{as} is the average particle diameter of seed. n_p is the number of particles being removed and n_s is the number of particles being added.
If $\ln(1 + P/S) = \ln(n_p/n_s) + 3\ln(D_{ap}/D_{as})$ holds true, then it implies that $n_p/n_s = 1$, which means no nucleation, agglomeration, or breakage is present. On the other hand $n_p/n_s < 1$ indicates that particle agglomeration takes place in the reactor and $n_p/n_s > 1$ means that particle breakage occurs in the pilot plant. The dashed lines in Figure 9 represent the analytical expression. The numerical results in Figure 9 agree with both analytical solution and experimental results which supports that the multi-scale model can be used for further control studies.

8. Operation and control

Bed temperature is one key factor for the deposition rate and the quality of the deposition. Inlet silane concentration also affect the deposition rate as well as fines formation and agglomeration. The fluidization mode is determined by a gas velocity ratio between superficial gas velocity u and minimum fluidization velocity u_{mf}. All these variables must be coordinated in a multi-variables process control strategy.
A careful selection of the fluidization velocity and silane concentration in the feed limit fines formation and agglomeration. In order to avoid slugging and poor gas-solid contact we adjust fluidization velocity or the ratio bed height to bed diameter during reactor design. Usually hydrogen is used as fluidization gas as it is able to decrease the formation of fines compared to other inert gas such as nitrogen.
Hsu *et al.* (Hsu et al., 1987) proposed that the optimal bed temperature for fluidized bed reactor is $600 - 700^oC$ and gas velocity ratio is between 3 and 5. Within this range, fines elutriation percentage is generally under 10% of the mass of Si in the silane feed. The maximum fine formation is 9.5% at the inlet silane concentration of 57%, no excessive fines

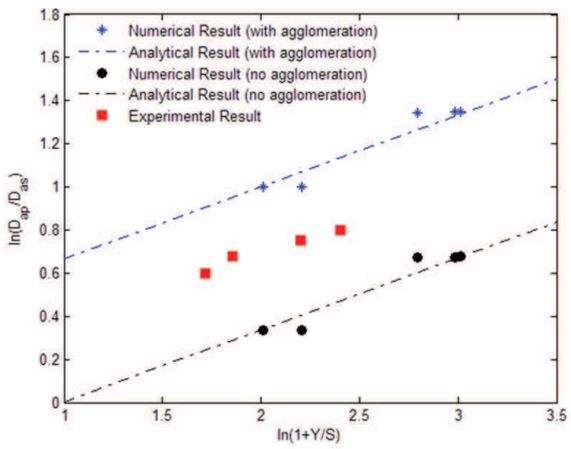

Fig. 9. Model Validation.

are generated with increasing silane concentration from 57% to 100%. Kojima *et al.* (Kojima & Morisawa, 1991) recommended the following operating conditions: bed temperature is 600^oC, gas velocity ratio is 4 and inlet silane concentration is 43%. For both groups, the recommended seed particle size is between 0.15 and 0.3 *melimeter*.

While considerable research effort has been devoted to understanding of the reaction mechanisms and model development for fluidized bed reactors, not much attention has been paid to the study of control technology for the silicon production process. Since this system is complex and typically have limited availability of measurements, complicated control strategies are not suitable to be implemented in the practice. Inventory control (Farschman et al., 1998) is a simple method for control of complex systems and thus has potential for industrial application. It distinguishes itself from other control methods in that it addresses the question of measurement and manipulated variables' selections. We apply inventory control strategy to control particle size distribution by manipulating the total mass of the particles.

The objective of our inventory control system is to control the average particle size in the fluidized bed reactor. We manipulate the seed and product flow rates to achieve the control objective. An inventory control strategy for the total mass hold-up of particles is written as:

$$\frac{dM}{dt} = -K(M - M^*) \tag{4}$$

where K is the proportional control gain. M is the total mass hold up and M^* is the desired hold up. The mass balance of the solid phase is expressed as:

$$\frac{dM}{dt} = S + Y - P \tag{5}$$

where S is the seed addition flow rate, Y is the silicon production rate and P is the product removal rate. The product flow rate can be manipulated to keep the total mass hold-up to a desired value M^* by using the following control action:

$$P = S + Y + K(M - M^*) \tag{6}$$

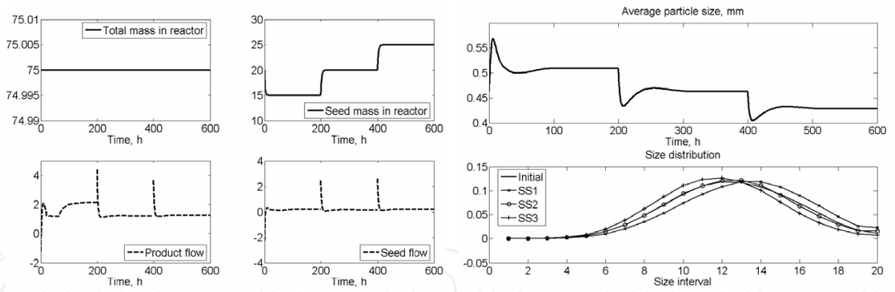

(a) Control total and seed hold up in FBR (b) Particle size using inventory control

Furthermore we apply inventory control to maintain the seed hold up to a desired value and the control action is in the form of

$$S = -\sum_{i=1}^{N_s} Y_i - K_s \left(\sum_{i=1}^{N_s} M_i - M^*_{\text{seed}} \right) \tag{7}$$

where N_s is the total number of size intervals for the particle seeds and Y_i is the silicon production rate in the seed size intervals, K_s is the proportional gain.
Simulation of controlling the total and seed particle hold-up is shown in Figures 10(a) and 10(b). The hold-up of particles in the system is shown in Figure 10(a). The product and seed flow rates required to achieve the control are also shown. The first steady state (SS1) represents operation when $M^*_{\text{total}} = 75$ and $M^*_{\text{seed}} = 15$. The subsequent steady states are achieved when M^*_{seed} is increased to 20 and 25. The average particle size and size distribution achieved during each steady state are shown in Figure 10(b). This simulation shows we can control the average product size as well as the product distribution. As the hold up of seed particles increases relative to the total hold up, the average size decreases. The interval representation of the size distribution supports this result. In this simulation, we assumed that the largest seed size interval, N_s, was interval 10 out of 20 and that the distribution of seed particles flowing into the system was constant.

9. Conclusions

This chapter reviewed the past and current work for modeling and operation of fluidized bed reactor processes for producing solar grade poly-silicon. Currently the shortage of low-cost solar grade silicon is one major factor preventing environmentally friendly solar energy from becoming important in the energy market. Energy consumption is the main cost driver for poly-silicon production process which is highly energy intensive. Fluidized bed reactors serve as an alternative to the Siemens process which dominates the solar grade silicon market. Several companies have attempted to commercialize the fluidized bed reactor process and the process has been scaled up to commercial scale. It has been shown that FBR technology produces poly-silicon at acceptable purity levels and an acceptable price. Extensive research has been carried out to study the chemical kinetics of silane pyrolysis and to model the fluid dynamics in the fluidized beds. The particle growth process due to silicon deposition is captured by discretized population balances which uses ordinary differential and algebraic equations to simulate the distribution function for the particles change as a function of time and operating conditions. A multi-scale modeling approach was applied to couple the population balance with computational fluid dynamics model and reaction model to represented the whole process. The model has been validated with experimental data from

pilot plant tests. An inventory based control is applied to control the total mass hold up of the solid phase and the simulation results demonstrate that such simple control strategy can be used to control the average particle size.

10. References

Abba, A., I., R. Grace, J. & T. Bi, H. (2002). Variable-gas-density fluidized bed reactor model for catalytic processes, *Chemical engineering science* 57(22-23): 4797–4807.

Balaji, S., Du, J., White, C. & Ydstie, B. (2010). Multi-scale modeling and control of fluidized beds for the production of solar grade silicon, *Powder Technology* 199(1): 23–31.

Cadoret, L., Reuge, N., Pannala, S., Syamlal, M., Coufort, C. & Caussat, B. (2007). Silicon cvd on powders in fluidized bed: Experimental and multifluid eulerian modelling study, *Surface and Coatings Technology* 201(22-23): 8919–8923.

Caussat, B., Hemati, M. & Couderc, J. (1995a). Silicon deposition from silane or disilane in a fluidized bed–part ii: Theoretical analysis and modeling, *Chemical engineering science* 50(22): 3625–3635.

Caussat, B., Hemati, M. & Couderc, J. (1995b). Silicon deposition from silane or disilane in a fluidized bed–part ii: Theoretical analysis and modeling, *Chemical engineering science* 50(22): 3625–3635.

Cavallaro, F. (2010). A comparative assessment of thin-film photovoltaic production processes using the electre iii method, *Energy Policy* 38(1): 463–474.

Cooper, D. & Clough, D. (1985). Experimental tracking of particle-size distribution in a fluidized bed, *Powder technology* 44(2): 169–177.

del Coso, G., del Canizo, C., Tobias, I. & Luque, A. (2007). Increase on siemens reactor throughput by tailoring temperature profile of polysilicon rods, *Electron Devices, 2007 Spanish Conference on*, IEEE, pp. 25–28.

Du, J., Balaji, S. & Ydstie, B. E. (2009). Multi-scale modeling and inventory control of particle growth processes, *9th International Symposium on Dynamics and Control of Process Systems*.

Farschman, C., Viswanath, K. & Erik Ydstie, B. (1998). Process systems and inventory control, *AIChE Journal* 44(8): 1841–1857.

Fishman, O. (2008). Solar silicon, *Advanced materials & processes* p. 33.

Goetzberger, A., Luther, J. & Willeke, G. (2002). Solar cells: past, present, future, *Solar energy materials and solar cells* 74(1-4): 1–11.

Green, M. & Emery, K. (1993). Solar cell efficiency tables, *Progress in Photovoltaics: Research and Applications* 1(1): 25–29.

Guenther, C., OŠBrien, T. & Syamlal, M. (2001). A numerical model of silane pyrolysis in a gas-solids fluidized bed, *Proceedings of the International Conference on Multiphase Flow*.

Henson, M. (2003). Dynamic modeling of microbial cell populations, *Current opinion in biotechnology* 14(5): 460–467.

Hogness, T., Wilson, T. & Johnson, W. (1936). The thermal decomposition of silane, *Journal of the American Chemical Society* 58(1): 108–112.

Hounslow, M. (1990). A discretized population balance for continuous systems at steady state, *AIChE journal* 36(1): 106–116.

Hsu, G., Levin, H., Hogle, R., Praturi, A. & Lutwack, R. (1982). Fluidized bed silicon deposition from silane. US Patent 4,314,525.

Hsu, G., Rohatgi, N. & Houseman, J. (1987). Silicon particle growth in a fluidized-bed reactor, *AIChE journal* 33(5): 784–791.

Hulburt, H. & Katz, S. (1964). Some problems in particle technology:: A statistical mechanical formulation, *Chemical Engineering Science* 19(8): 555–574.

Iya, S., Flagella, R. & DiPaolo, F. (1982). Heterogeneous decomposition of silane in a fixed bed reactor, *Journal of The Electrochemical Society* 129: 1531.

Kojima, T. & Morisawa, O. (1991). Optimum process conditions for stable and effective operation of a fluidized bed cvd reactor for polycrystalline silicon production.

Kunii, D. & Levenspiel, O. (1991). *Fluidization engineering*, Vol. 101, Butterworth-Heinemann Boston.

Lai, S., Dudukovic, M. & Ramachandran, P. (1986). Chemical vapor deposition and homogeneous nucleation in fluidized bed reactors: silicon from silane, *Chemical Engineering Science* 41(4): 633–641.

Mahecha-Botero, A., Grace, J., Elnashaie, S. & Lim, C. (2005). Femlab simulations using a comprehensive model for gas fluidized-bed reactors, *COMSOL Multiphysics (FEMLAB) Conference Proceedings, Boston, USA*.

Mahecha-Botero, A., Grace, J., Elnashaie, S. & Lim, C. (2006). Comprehensive modeling of gas fluidized-bed reactors allowing for transients, multiple flow regimes and selective removal of species, *International Journal of Chemical Reactor Engineering* 4(4): 11.

Muller, A., Ghosh, M., Sonnenschein, R. & Woditsch, P. (2006). Silicon for photovoltaic application, *Materials Science and Engineering* 134: 257–262.

Muller, M., Birkmann, B., Mosel, F., Westram, I. & Seidl, A. (2010). Silicon efg process development by multiscale modeling, *Journal of Crystal Growth* 312(8): 1397–1401.

Neuhaus, D. & Münzer, A. (2007). Industrial silicon wafer solar cells, *Advances in OptoElectronics, ID* 24521.

Odden, J., Egeberg, P. & Kjekshus, A. (2005). From monosilane to crystalline silicon, part i: Decomposition of monosilane at 690-830ák and initial pressures 0.1-6.6 ámpa in a free-space reactor, *Solar energy materials and solar cells* 86(2): 165–176.

Piña, J., Bucalá, V., Schbib, N., Ege, P. & De Lasa, H. (2006). Modeling a silicon cvd spouted bed pilot plant reactor, *International Journal of Chemical Reactor Engineering* 4(4): 9.

Randolph, A. & Larson, M. (1971). *Theory of particulate processes*, Academic Press.

Steinbach, I., Apel, M., Rettelbach, T. & Franke, D. (2002). Numerical simulations for silicon crystallization processes–examples from ingot and ribbon casting, *Solar energy materials and solar cells* 72(1-4): 59–68.

Surek, T. (2005). Crystal growth and materials research in photovoltaics: progress and challenges, *Journal of Crystal Growth* 275(1-2): 292–304.

Talalaev, R. (2009). Polysim: Modeling of polysilicon deposition by siemens process, *International Semiconductor Technology Conference*.

White, C. (2007). Modeling for design and control of particulate systems.

White, C., Ege, P. & Erik Ydstie, B. (2006). Size distribution modeling for fluidized bed solar-grade silicon production, *Powder technology* 163(1-2): 51–58.

White, C., Zeininger, G., Ege, P. & Ydstie, B. (2007). Multi-scale modeling and constrained sensitivity analysis of particulate cvd systems, *Chemical Vapor Deposition* 13(9): 507–512.

Woditsch, P. & Koch, W. (2002). Solar grade silicon feedstock supply for pv industry, *Solar energy materials and solar cells* 72(1-4): 11–26.

Würfel, P. (2005). *Physics of solar cells: from principles to new concepts*, Vch Verlagsgesellschaft Mbh.

Zambov, L. (1992). Kinetics of homogeneous decomposition of silane, *Journal of crystal growth* 125(1-2): 164–174.

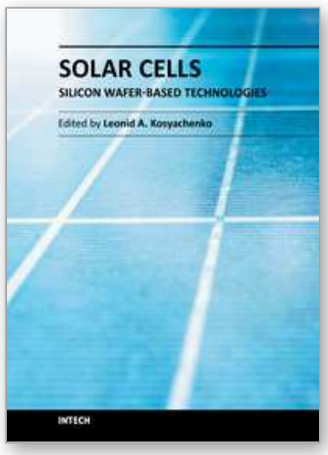

Solar Cells - Silicon Wafer-Based Technologies

Edited by Prof. Leonid A. Kosyachenko

ISBN 978-953-307-747-5
Hard cover, 364 pages
Publisher InTech
Published online 02, November, 2011
Published in print edition November, 2011

The third book of four-volume edition of 'Solar Cells' is devoted to solar cells based on silicon wafers, i.e., the main material used in today's photovoltaics. The volume includes the chapters that present new results of research aimed to improve efficiency, to reduce consumption of materials and to lower cost of wafer-based silicon solar cells as well as new methods of research and testing of the devices. Light trapping design in c-Si and mc-Si solar cells, solar-energy conversion as a function of the geometric-concentration factor, design criteria for spacecraft solar arrays are considered in several chapters. A system for the micrometric characterization of solar cells, for identifying the electrical parameters of PV solar generators, a new model for extracting the physical parameters of solar cells, LBIC method for characterization of solar cells, non-idealities in the I-V characteristic of the PV generators are discussed in other chapters of the volume.

InTech Europe
University Campus STeP Ri
Slavka Krautzeka 83/A
51000 Rijeka, Croatia
Phone: +385 (51) 770 447
Fax: +385 (51) 686 166
www.intechopen.com

InTech China
Unit 405, Office Block, Hotel Equatorial Shanghai
No.65, Yan An Road (West), Shanghai, 200040, China
中国上海市延安西路65号上海国际贵都大饭店办公楼405单元
Phone: +86-21-62489820
Fax: +86-21-62489821

IntechOpen